# Designed Replacement of an Internal Hydration Water Molecule in BPTI: Structural and Functional Implications of a Glycine-to-Serine Mutation†

Kurt D. Berndt,‡ Jürgen Beunink,§ Werner Schröder,∥ and Kurt Wüthrich*,‡

*Institut für Molekularbiologie und Biophysik, Eidgenössische Technische Hochschule-Hönggerberg, CH-8093 Zürich, Switzerland, Bayer AG, Verfahrensentwicklung Biochemie, Friedrich Ebert Strasse 217, D-5600 Wuppertal, Germany, and Bayer AG, Institut für Herz-, Kreislauf-, und Arteriosklerose-Forschung, Aprather Weg 18, D-5600 Wuppertal, Germany*

*Received November 2, 1992; Revised Manuscript Received February 3, 1993*

ABSTRACT: The three-dimensional structure of the basic pancreatic trypsin inhibitor (BPTI) contains four internal water molecules, which form a total of nine intermolecular hydrogen bonds with the BPTI polypeptide chain. To investigate the effect of such internal hydration on protein structure and stability, we displaced one of the internal water molecules in a recombinant BPTI analogue, BPTI(G36S), in which Gly 36 is replaced by serine. The replacement of a water molecule by the seryl side chain was established by the absence of the protein–water nuclear Overhauser effects (NOE) that had been attributed to the water molecule near Gly 36 in wild-type BPTI and by the presence of new, intramolecular NOEs to the hydroxyl proton of Ser 36. BPTI(G36S) has slightly reduced thermal stability compared to BPTI, corresponding to a destablization by $\Delta(\Delta G) \approx 0.7$ kcal/M in 6 M guanidinium hydrochloride solution. Additionally, the stabilities of the complexes formed between BPTI(G36S) and trypsin, plasmin, or kallikrein are significantly reduced when compared to the corresponding complexes with wild-type BPTI.

Water has long been recognized as having a profound effect on protein structure, function, and stability. Its ability to form extensive hydrogen bond networks underlies the hydrophobic effect, which has been proposed to be a dominant force in determining protein stability (e.g., Kauzmann, 1959; Tanford, 1962; Némethy & Scheraga, 1977; Dill, 1987). Although water is generally excluded from the predominantly apolar interior of globular proteins, a small number of water molecules are sometimes found to be an integral part of the molecular architecture, being isolated from the bulk solvent, highly conserved in homologous proteins, and invariably hydrogen-bonded to polar or charged groups of the polypeptide chain (Baker & Hubbard, 1984). Similarly, "interior water" is sometimes observed at the interface between associating biological macromolecules, where it may have important roles in both intermolecular recognition and stability of the complexes formed (Otwinowski et al., 1988). Until recently, the observation of interior hydration water has been limited to X-ray diffraction studies with protein crystals. Such crystal data can now be complemented by NMR[1] studies in solution (Otting & Wüthrich, 1989). NMR experiments with several proteins have shown that interior waters observed in protein crystals are usually conserved in solution (Otting & Wüthrich, 1989; Clore et al., 1990; Forman-Kay et al., 1991), and the crystallographic information was supplemented by the observation that interior hydration water molecules exchange with the bulk water on a millisecond time scale or faster (Otting et al., 1991a). To further investigate the structural and functional roles of internal hydration, this paper compares the wild-type form of a protein with a recombinant mutant form in which a single internal water molecule was replaced by a serine side chain.

The crystal structure of the basic pancreatic trypsin inhibitor (BPTI) contains four interior water molecules, which form a total of nine protein–water and two water–water hydrogen bonds (Deisenhofer & Steigemann, 1975; Wlodawer et al., 1984, 1987). These four water molecules are located in two regions of the molecule (Figure 1). The single water molecule W122 is enclosed by the two loops containing the amino acids residues 11–14 and 36–38 (top of Figure 1). A cluster formed by the three water molcules W111, W112, and W113 is in an interior channel surrounded by residues 8–10 and 40–44 (center of Figure 1). These interior water molecules are all inaccessible to the bulk solvent and were found in the same locations in the NMR solution structure of BPTI (Otting & Wüthrich, 1989; Berndt et al., 1992). We have recently extended our studies of Kunitz-type proteinase inhibitors by a structure determination of the dendrotoxin K from the venom of *Dendroaspis polylepis polylepis* (Berndt et al., 1993). Although this protein has only 42% sequence identity with BPTI (Figure 2), the three-dimensional structures of the two proteins are virtually identical. Nonetheless, toxin K shows only negligible binding to known proteases (Strydom, 1973), and its denaturation temperature, $T_m$, in $H_2O$ at pH 4.6 is 57 °C, as compared to $T_m > 90$ °C for BPTI. Toxin K contains Ser in position 36 (Figure 2), and this residue was found to

† This work was supported by the Schweizerischer Nationalfonds (Project 31.32033.91).

* Author to whom correspondence should be addressed.
‡ Institut für Molekularbiologie und Biophysik.
§ Bayer AG, Verfahrensentwicklung Biochemie.
∥ Bayer AG, Institut für Herz-, Krieslauf-, und Arteriosklerose-Forschung.

[1] Abbreviations: BPTI, bovine pancreatic trypsin inhibitor; toxin K, dendrotoxin K (or "trypsin inhibitor homologue K") from the venom of the black mamba, *Dendroaspis polylepis polylepis*; BPTI(G36S), BPTI having Gly 36 replaced by Ser; TPCK, *N*-tosyl-L-phenylalanine chloromethyl ketone; SDS, sodium dodecyl sulfate; PAGE, polyacrylamide gel electrophoresls; RP-HPLC, reverse-phase high-performance liquid chromatography; TFA, trifluoroacetic acid; NMR, nuclear magnetic resonance; 2D, two dimensional; 2QF-COSY, 2D two-quantum-filtered correlation spectroscopy; TOCSY, 2D total correlation spectroscopy; NOE, nuclear Overhauser effect; NOESY, 2D NOE spectroscopy; $^3J_{HN\alpha}$, vicinal spin–spin coupling constant between the amide proton and the $\alpha$-proton; $^3J_{\alpha\beta}$, vicinal spin–spin coupling constant between the $\alpha$-proton and a $\beta$-proton; $^3J_{BH\gamma OH}$, vicinal spin–spin coupling constant between the $\beta$-proton and a $\gamma$-hydroxyl proton in Ser or Thr.

0006-2960/93/0432-4564$04.00/0 

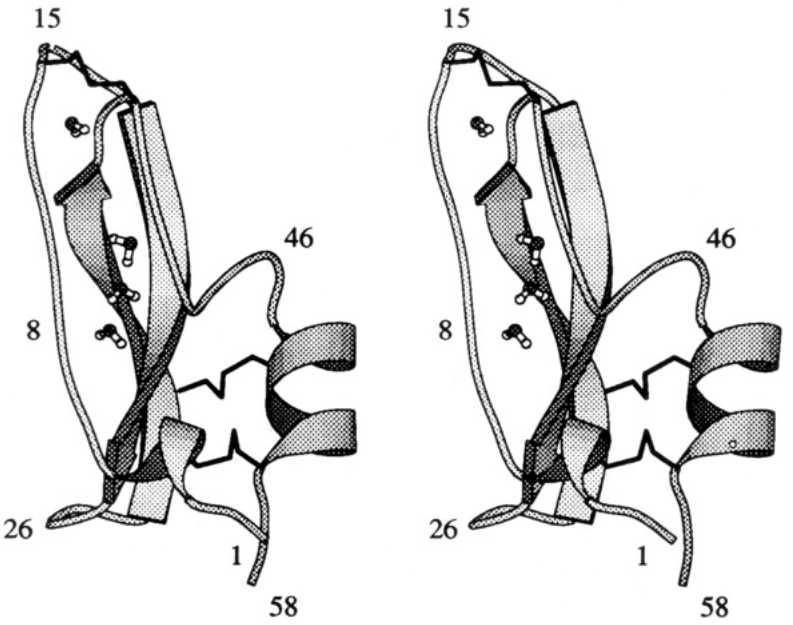


FIGURE 1: Stereoview of a cartoon of the X-ray crystal structure of BPTI form II (Wlodawer et al., 1984) produced with the program Molscript (Kraulis, 1991). The four internal water molecules W122, W113, W112, and W111 (from top to bottom) are drawn as ball-and-stick models. The three disulfide bonds 14–38, 30–51, and 5–55 (from top to bottom) are traced with thick black lines. The same molecular architecture has been observed for BPTI in solution (Berndt et al., 1992; Otting & Wüthrich, 1989). In BPTI(G36S) and toxin K, the water molecule W122 is replaced by the Ser 36 side chain (Berndt et al., 1993). The numbers on the outside of the structure identify selected sequence locations.

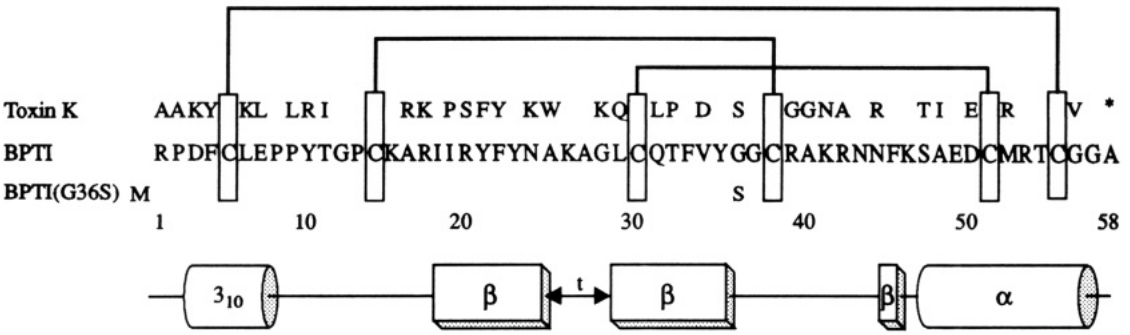


FIGURE 2: Comparison of the amino acid sequences of BPTI, toxin K, and BPTI(G36S). The complete sequence of BPTI is shown, and for toxin K and BPTI(G36S) only those residues are listed which are different from BPTI. The sequence numbers are those of BPTI. Toxin K contains only 57 residues. BPTI(G36S) contains an additional Met residue in position 0. Boxes are drawn around the six Cys residues, and the disulfide pairings are indicated by lines connecting the boxes. The secondary structure, which is common to all three species, is shown below the sequence, where "$3_{10}$" identifies to $3_{10}$-helix, "$\beta$" the individual strands of an antiparallel $\beta$-sheet, "t" a tight turn, and "$\alpha$" an $\alpha$-helix.

displace the water molecule W122 located near Gly 36 in BPTI (Figure 1). In order to assess the contributions of this structural difference to the altered stability and functional properties of toxin K, we prepared the mutant BPTI(G36S), which differs from wild-type BPTI only by the substitution of Gly 36 by Ser. This paper describes structural studies of BPTI(G36S) by NMR as well as measurements of its thermal stability and binding affinity to serine proteases.

## MATERIALS AND METHODS

*Materials.* Human plasmin and human plasma kallikrein were purchased from Protogen (Läufelfingen, Switzerland). TPCK-treated bovine trypsin was purchased from Worthington. The substrates used for proteinase assays were as follows: for plasma kallikreine, H-D-Pro-Phe-Arg *p*-nitroanilide (Nova Biochem); for plasmin, *N*-*p*-tosyl-Gly-Pro-Lys *p*-nitroanilide (Sigma); for trypsin, Pyrglu-Arg *p*-nitroanilide (Pharmacia). Stock solutions of guanidine·HCl (Ultrapure, BRL) containing 5 mM citrate were adjusted to pH 4.6, and their final concentrations were determined by refractive index (Nozaki, 1972). All other chemicals were of the highest purity obtainable.

*Preparation of Recombinant $^{15}N$-Labeled BPTI(G36S).* The protein BPTI(G36S) was produced in a mutant derivative of *Saccharomyces cerevisiae*, strain JC 34.4 D. The yeast strain and the expression vector used are described in detail in Das et al. (1989). The G36S exchange in the BPTI gene was carried out by oligonucleotide mutagenesis on a synthetic BPTI gene, employing yeast-preferred codons. Vector construction, cloning, and transformation of the yeast cells were carried out using standard gene technology methods (Sambrook et al., 1989). The transformed yeast cells were grown in chemically defined media containing 97% $^{15}N$-enriched $(NH_4)_2SO_4$ as the sole nitrogen source. The correctly folded BPTI(G36S) secreted by the cells was purified from the cell-free culture broth using conventional ion-exchange chromatography and $C_{18}$ RP-HPLC. The purified protein was lyophilized and characterized by SDS–PAGE, analytical RP-HPLC, and N-terminal sequencing. Comparison of $^1H$ NMR spectra recorded before and after the HPLC purification step showed that the protein structure was not noticeably affected by the HPLC treatment.

*Monitoring Thermal Unfolding and Refolding.* Circular dichroism (CD) spectra were obtained with a Jasco J-710

spectropolarimeter using thermostated cuvettes with 0.1-cm path length (Helma). For all experiments, the temperature was controlled to 0.05 °C with an Endocal RTE-100 FRC circulating bath (Neslab). Because of the high thermostability of BPTI in aqueous solution (denaturation temperature, $T_m$, >90°C), thermodynamic parameters were derived from spectroscopic unfolding curves recorded in the presence of a denaturant (Brown et al., 1978). Guanidine·HCl was chosen as the denaturant, since it appears to have little if any effect on the overall structure of BPTI at temperatures between 15 and 40 °C. This was concluded from the observation that the molar ellipticity at 220 nm decreased linearly with increasing concentration of guanidine·HCl between 0 and 6 M. The fraction of native structure during thermal unfolding was monitored by CD at 220 nm. Equilibrium constants were determined from these data following a linear least-squares analysis of the pre- and posttransition regions. The slope of the van't Hoff plot (ln $K$ versus $^1/_T$) was determined using the data collected within a range of 6 °C centered about the melting temperature, $T_m$. No attempts were made to reduce the three disulfide bonds of BPTI, and therefore our use of the term "unfolded form" refers to states where the native conformation, as monitored by CD, has been lost without breaking the native disulfide bonds.

*Nuclear Magnetic Resonance Experiments.* NMR spectra were recorded from samples of 10 mM toxin K or 15 mM BPTI(G36S), either in a mixture of 95% $H_2O$/5% $^2H_2O$ or in 99.99% $^2H_2O$ after complete exchange of all labile protons. The protein samples were adjusted to pH 4.6 by the addition of minute amounts of NaOH and HCl, or NaO$^2$H and $^2$HCl, respectively, and the temperature was regulated to ±0.5 °C. The NMR spectra were recorded on either a Bruker AM500 or AM600 spectrometer using the phase-sensitive mode with time-proportional phase incrementation of the initial pulse (Marion & Wüthrich, 1983). Quadrature detection was used in both dimensions, with the carrier placed in the center of the spectrum. $^1$H and $^{15}$N NMR assignments of BPTI(G36S) were made using 2D heteronuclear [$^{15}$N,$^1$H]-TOCSY and 2D homonuclear [$^1$H,$^1$H]-NOESY experiments recorded at 4 °C. Protein–water NOEs were identified from 2D homonuclear [$^1$H,$^1$H]-NOESY experiments using a selective spin lock to suppress the water signal (Otting et al., 1991b). Time-domain data were processed on a Bruker X-32 data station using UXNMR software. The NOESY spectra were weighted with a cosine window and zero-filled and 2-fold in both dimensions prior to Fourier transformation. Baseline distortions in NOESY spectra were eliminated using the FLATT procedure (Güntert & Wüthrich, 1992).

*Binding Affinity of BPTI and BPTI(G36S) to Proteinases.* Enzyme inhibition was assayed by measuring the hydrolytic activities in several series of preincubated samples, each of which contained the same amount of proteinase and variable amounts of inhibitor. Also included was a reference sample without inhibitor. Preincubations were carried out for 3–18 h, depending on the combinations of enzyme and inhibitor and the enzyme concentration used. The residual enzyme activities were determined spectrophotometrically using a Microplate (Dynatech) reader at 405 nm, with the absorbance at 490 nm as a reference. The enzyme concentrations were calculated on the basis of 1:1 stoichiometric inhibition obtained with known concentrations of good inhibitors for these proteinases. The inhibitor concentrations in the samples used for the binding studies were calculated from amino acid analyses performed with the samples containing both the enzyme and the inhibitor. The $K_i$ values of the enzyme–inhibitor complexes were calculated from the titration curves according to the method of Empie and Laskowski (1982).

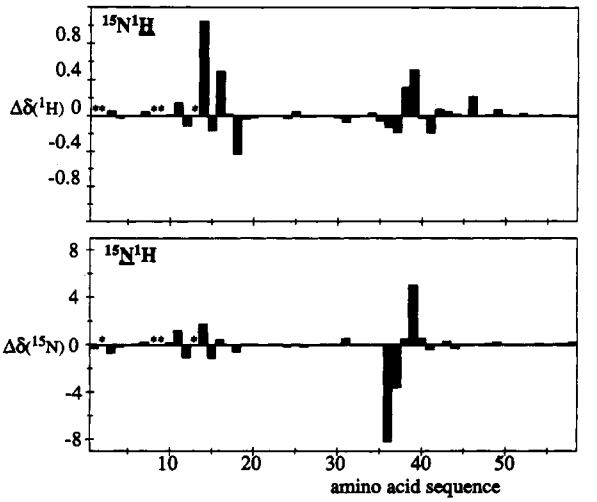


FIGURE 3: Amide proton and amide $^{15}$N chemical shift differences between BPTI and BPTI(G36S), $\Delta\delta = \delta$(BPTI) – $\delta$(BPTI(G36S)), at 4 °C and pH 4.6, plotted versus the amino acid sequence. Asterisks denote missing data at residue positions 1, 2, 8, 9, and 13, where the residues 2, 8, 9, and 13 are Pro.

## RESULTS AND DISCUSSION

*Sequence-Specific NMR Assignments for BPTI(G36S) and Structural Comparison with BPTI.* A nearly complete list of sequence-specific $^1$H and $^{15}$N NMR assignments have been determined for BPTI(G36S). This procedure was facilitated by the facts that complete assignments at 4 °C had previously been obtained for BPTI (G. Otting and K. Wüthrich, unpublished) and that there is close similarity of chemical shifts between corresponding residues in BPTI and BPTI(G36S) at 4 °C. Significant differences between corresponding amide nitrogen and amide proton chemical shifts exist for only a few residues (Figure 3). These are located in two spatially adjacent loops formed by the residues 11–18 and 34–41, of which one contains the point mutation G36S (Figures 1 and 2). The close similarity in chemical shifts between the two proteins is highly suggestive of an overall similar three-dimensional structure (Wüthrich, 1976, 1986). Furthermore, it is noteworthy that the unusual high-field shifts of the backbone amide proton of Gly 37 and one side chain amide proton of Asn 44 in BPTI (Berndt et al., 1992; Tüchsen & Woodward, 1987) are also observed in the mutant BPTI(G36S).

*Studies of the Local Structure of BPTI(G36S) near Residue 36.* Hydroxyl protons of serine and threonine are known to have intrinsically different chemical shifts from that of water (Liepinsh et al., 1992). Separate signals are usually not observed in standard NMR experiments due to the rapid exchange of these protons with the solvent, which averages out the chemical shift difference between the hydroxyl protons and the water (Chazin & Wright, 1988; Liepinsh et al., 1992; Otting & Wüthrich, 1989). In $H_2O$ solutions of BPTI(G36S) the hydroxyl proton resonance of Ser 36 is, however, observed as a separate line with a chemical shift of 5.27 ppm. The resonance assignment was based on the observation of intraresidual cross peaks with $H^{\beta 2}$ and $H^{\beta 3}$ in a 2QF-COSY spectrum and with HN, $H^{\alpha}$, $H^{\beta 2}$, and $H^{\beta 3}$ in TOCSY spectra recorded in $H_2O$.

Solvent suppression schemes using one or multiple spin-lock pulses have permitted the observation of intermolecular NOEs between water protons and polypeptide protons (Otting

Table I: Short $^1H$–$^1H$ Distances in the Crystal Structure of BPTI Form II and Corresponding NOEs with the Water Molecule W122 (Figure 1) in Aqueous BPTI Solution, or with the Hydroxyl Proton of Ser 36 in BPTI(G36S) or in Toxin K, Respectively

| | proteins compared[b] | | | |
|---|---|---|---|---|
| hydrogen atoms[a] | 5PTI W122 ($d$ < 4.0 Å) | BPTI $H_2O$ (NOE) | BPTI(G36S) Ser 36 γOH (NOE) | toxin K Ser 36 γOH (NOE) |
| Thr(I) 11 Hα | | | | + |
| Thr(I) 11 $C^{\gamma}H_3$ | + | + | + | + |
| Gly 12 $H\alpha_1$ | | + | + | + |
| Gly 12 $H\alpha_2$ | + | + | + | + |
| Pro 13 $H\delta_2$ | + | + | | + |
| Cys 14 HN | + | + | + | + |
| Cys 14 $H\beta_2$ | + | | | + |
| Tyr 35 $H\delta_1$ | + | + | + | + |
| Tyr 35 $H\epsilon_1$ | + | | + | + |
| Gly 36 $H\alpha_1$ | + | + | | |
| Gly 36 $H\alpha_2$ | + | + | | |
| Ser 36 HN | | | + | + |
| Ser 36 Hα | | | + | + |
| Ser 36 $H\beta_2$ | | | + | + |
| Ser 36 $H\beta_3$ | | | + | + |
| Gly 37 HN | + | + | + | + |
| Cys 38 HN | + | + | + | + |

[a] The residues given by three-letter symbols correspond to the sequences of BPTI and BPTI(G36S) (Figure 2). Residue replacements in toxin K are indicated in parentheses, using the one-letter amino acid code. [a] The first row gives the same of the protein, where 5PTI refers to the Brookhaven Data Bank code for the crystal structure of BPTI form II (Wlodawer et al., 1984). The second row identifies the water molecule W122 in the crystal structure and the corresponding groups in the other structures. The third row indicates the data represented by the "+" signs in the table, i.e., a polypeptide proton–water proton distance shorter than 4.0 Å in the crystal structure, or the presence of a NOE with the water molecule or with Ser 36 OH in the protein solutions. The boxes indicate that the corresponding atoms do not exist in the proteins outside of the box. The NOE data on BPTI are from Otting and Wüthrich (1989); those on toxin K are from Berndt et al. (1993).

& Wüthrich, 1989; Otting et al., 1991b). Using these techniques, all four internal water molecules originally identified in the X-ray crystal structures of BPTI (Deisenhofer & Steigemann, 1975; Wlodawer et al., 1984, 1987) had been identified in the same locations in the solution structure. Similar studies with the mutant protein showed that all of the intermolecular NOEs attributed to the internal water molecule W122 in BPTI (Table I) are absent in corresponding spectra recorded with BPTI(G36S). This result coincides with previous observation for toxin K, where it has been established that the hydroxyl group of Ser 36 replaces the water molecule W122 and is engaged in three of the four hydrogen bonds attributed to W122 in wild-type BPTI (Berndt et al., 1993). In contrast, similar patterns of intermolecular NOEs with the cluster of the three water molecules W111, W112, and W113 (Figure 1) were found in BPTI and BPTI(G36), showing that these three internal hydration water molecules are conserved in the mutant protein in spite of the amino acid replacement in position 36.

The fact that the hydroxyl proton resonance of Ser 36 was observed, even under conditions of preirradiation of the solvent resonance in conventional 2QF-COSY, TOCSY, and NOESY spectra in $H_2O$ solution, implies low solvent acessibility and the likely participation of this proton in at least one intramolecular hydrogen bond. This in turn should result in a number of NOE cross peaks to neighboring protons. In fact, a total of 12 intramolecular protein–protein NOEs (four intraresidual, three sequential, and five longer-range) with this hydroxyl proton were found in BPTI(G36S) (Figure 4, panels B and B′; Table I). When one compares the intramolecular protein–protein NOEs in BPTI(G36S) with the intermolecular protein–water NOEs observed in BPTI, one finds that nearly all protons giving rise to NOE cross peaks with the water molecule W122 in BPTI are also involved in cross peaks to the hydroxyl proton of Ser 36 in the mutant protein. In addition, nearly all the intramolecular NOEs involving the hydroxyl proton of Ser 36 in spectra of BPTI(G36S) are also present in NOESY spectra of toxin K (Table I), where they also have similar relative intensities (Figure 4, panels A and A′). These data, combined with the observation that the protein protons which interact with the hydroxyl proton of Ser 36 do not give rise to cross peaks with the water resonance in either BPTI(G36S) or toxin K, show convincingly that the hydroxyl group of Ser 36 in the mutant protein occupies the same position as the water molecule W122 in BPTI.

*Hydrogen Bonds with Ser 36 OH in BPTI(G36S).* To investigate the hydrogen-bonding patterns of Ser 36 in the mutant BPTI, we chose the indirect approach of analyzing the previously determined structures of BPTI and toxin K near amino acid residue 36 and then evaluating this region of the structure of toxin K in the light of the experimental data of BPTI(G36S).

The hydrogen-bonding network which involves the water molecule W122 in the X-ray crystal structure of BPTI form II (Wlodawer et al., 1984) (Figure 5A) includes interactions with the backbone amide protons of Cys 14 and Cys 38 acting as proton donors and the two backbone carbonyl oxygens of Thr 11 and Cys 38 participating as acceptors. The criteria used in this identification of hydrogen bonds are that the proton–acceptor distance must be less than 2.4 Å and that the angle between the donor–proton bond and the line connecting the donor and acceptor atoms must be less than 35°. A very similar pattern of hydrogen bonds is seen in toxin K (Figure 5B), where the hydroxyl oxygen of Ser 36 serves as the acceptor for the amide protons of Cys 38 and Cys 14, and the hydroxyl proton of Ser 36 forms a hydrogen bond with the carbonyl oxygen of Ile 11. Compared to BPTI, this scheme leaves the carbonyl oxygen of Cys 38 as an unsatisfied potential hydrogen-bond acceptor, since the serine side chain does not contain a counterpart to the water proton associated with this carbonyl group. The hydrogen bond between the amide proton of Cys 38 and the hydroxyl oxygen of Ser 36 deserves special attention. Using the aforementioned standard criteria for hydrogen bond identification, it is found in only nine of the 20 NMR conformers used to represent the solution structure of toxin K (Berndt et al., 1993). Of the nine conformers forming the HN Cys 38–γO Ser 36 hydrogen bond, eight have a "left-handed" 14–38 disulfide chirality (Richardson, 1981), while eight of the other 11 conformers possess "right-handed" disulfides. For comparison with BPTI, where only the "right-handed" 14–38 disulfide chirality was reported for all three X-ray crystal structures, a conformer of toxin K containing a right-handed disulfide is shown in Figure 5B. Formation of the right-handed disulfide chirality pulls the amide proton of Cys 38 away from the hydroxyl oxygen of Ser 36 by up to 0.6 Å, thus weakening or perhaps even breaking this hydrogen bond.

Returning now to the structure of BPTI(G36S), Table I shows that seven of the eight intermolecular protein–water NOEs with W122 identified in BPTI, for which the corresponding polypeptide atoms are also present in the mutant protein, have intramolecular counterparts in BPTI(G36S). All of these NOEs are also present in spectra of toxin K (Table I). Furthermore, the relative intensities of the NOEs to the hydroxyl proton in BPTI(G36S) are very similar to those of the corresponding NOEs in toxin K (Figure 4). The spatial

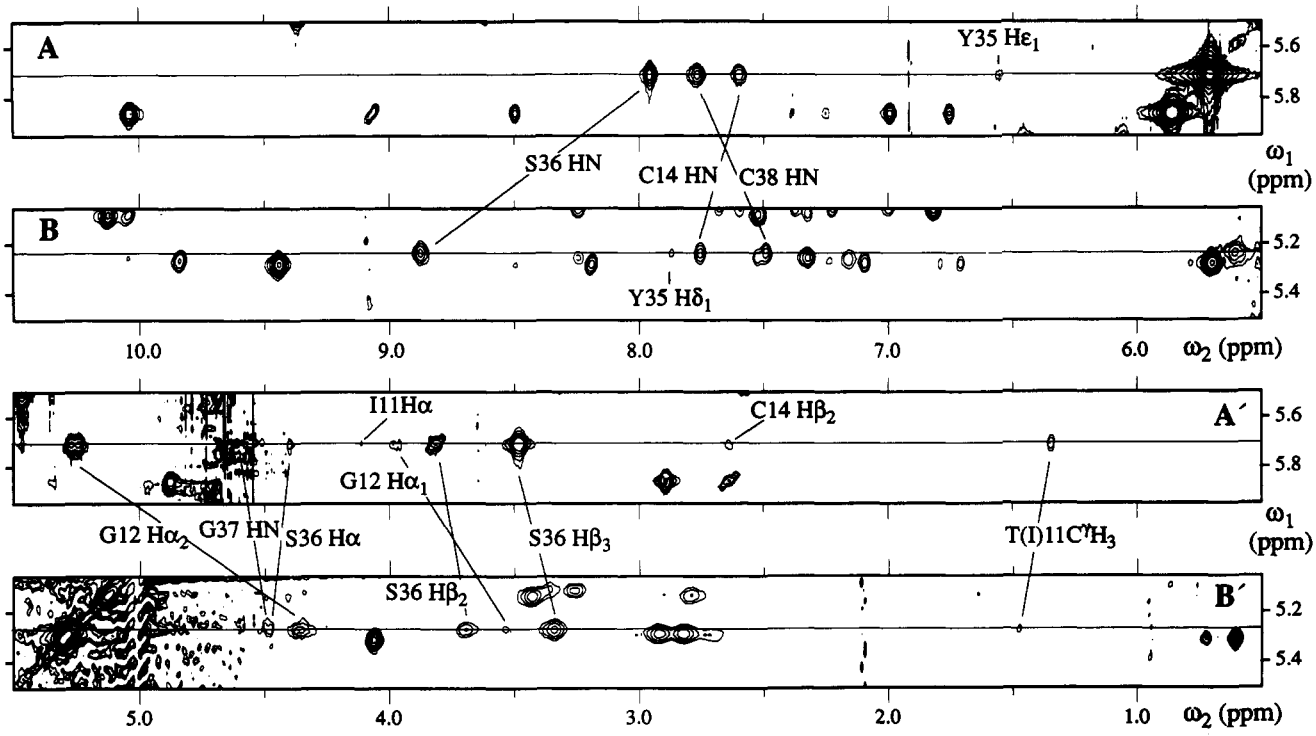


FIGURE 4: Contour plots of spectral regions from [$^1$H,$^1$H]-NOESY spectra of toxin K and BPTI(G36S) showing the NOE cross peaks involving the hydroxyl proton of Ser 36. Both spectra were recorded at 600 MHz in a mixed solvent of 95% $H_2O$/5% $^2H_2O$ at pH 4.6; for toxin K the concentration was 10 mM, the mixing time $\tau_m$ = 40 ms, and $T$ = 36 °C; for BPTI(G36S) the concentration was 20 mM, $\tau_m$ = 25 ms, and $T$ = 4 °C. (A) Toxin K, $\omega_1$ = 5.50–5.95 ppm, $\omega_2$ = 5.50–10.50 ppm. (A′) Toxin K, $\omega_1$ = 5.50–5.95 ppm, $\omega_2$ = 0.50–5.50 ppm. (B) BPTI(G36S), $\omega_1$ = 5.05–5.50 ppm, $\omega_2$ = 5.50–10.50 ppm. (B′) BPTI(G36S), $\omega_1$ = 5.05–5.50 ppm, $\omega_2$ = 0.50–5.50 ppm. In each spectrum a thin horizontal line indicates the $\omega_1$ chemical shift of Ser 36 OH. Cross peaks with this resonance are identified with the one-letter amino acid symbol, the sequence number, HN for backbone amide protons, or a greek letter indicating other proton positions and, where applicable, a number for the stereospecific assignment. Amino acid substitutions in toxin K are shown in parentheses. Where corresponding NOEs were observed in the two proteins, a line connects the cross peaks in the two spectra.

Table II: Thermodynamic Parameters for Thermal Unfolding of Wild-Type BPTI and BPTI(G36S) in 6 M Guanidinium Hydrochloride[a]

| protein | $T_m$[b] (°C) | $\Delta T_m$[c] (°C) | $\Delta S_m$[d] (cal/deg·mol) | $\Delta H_m$[e] (kcal/mol) | $\Delta(\Delta G)_m$[f] (kcal/mol) |
|---|---|---|---|---|---|
| BPTI | 72.6 ± 0.2 | | 148 ± 11 | 51 ± 3 | |
| BPTI(G36S) | 67.9 ± 0.2 | 4.5 ± 0.3 | 149 ± 8 | 51 ± 2 | 0.7 ± 0.1 |

[a] Derived from van't Hoff analyses of the reversible thermal denaturation of wild-type BPTI and BPTI(G36S) in the presence of 6 M guanidinium chloride as measured by CD at 220 nm. Values of $\Delta S_m$ and $\Delta H_m$ are given for the unfolding reaction. [b] Determined from the slope of a plot of $\Delta G$ versus $T$ at $T_m$. [c] $\Delta T_m$ is the difference between the $T_m$ values of the two proteins. [d] Determined from the slope of a plot of $\Delta G$ versus $T$ at $T_m$. [e] $\Delta H_m = T_m \Delta S_m$. [f] $\Delta(\Delta G)_m = \Delta T_m \Delta S_m^N = \Delta T_m(\Delta H_m^N/T_m^N)$, where $\Delta S_m^N$, $\Delta H_m^N$, and $T_m^N$ are the parameter values for native BPTI.

orientation of the hydroxyl proton of Ser 36 was directly determined in BPTI(G36S) from measurements of NOEs and coupling constants between the hydroxyl proton and the β-protons, using the same NMR techniques as described recently for BPTI (Liepinsh et al., 1992). The γOH–βH 2QF-COSY cross-peak patterns in $H_2O$ indicate that there is a small and a large coupling constant $^3J_{\beta H\gamma OH}$, with the hydroxyl proton showing a stronger NOE to the $\beta_3$-proton. This coincides exactly with the observations in toxin K, for which the hydroxyl orientation is well-determined in the solution structure (Berndt et al., 1993). Overall, the similar patterns and intensities of the NOEs with the hydroxyl proton of Ser 36 in BPTI(G36S) and in toxin K show that the structure of the molecular region of toxin K shown in Figure 5 must indeed be very similar to the corresponding region of BPTI-(G36S).

*Denaturation Studies of BPTI(G36S).* The CD spectra of BPTI and BPTI(G36S) recorded at pH 4.6 over the temperature range 20–90 °C are nearly superimposable throughout the region 180–350 nm, implying that the secondary structure and the high thermostability exhibited by BPTI are preserved in BPTI(G36S). The mutant protein was also found, like BPTI, to be resistant to denaturation by 6 M guanidinium hydrochloride at ambient temperature. Stability curves obtained in the presence of 6 M guanidinium hydrochloride yielded a midpoint of the thermal transition, $T_m$, of 72.6 °C for BPTI and 67.8 °C for BPTI(G36S) (Table II). From analysis of the thermal unfolding curves using a two-state approximation (Becktel & Schellman, 1987), the difference in stability between the two proteins, $\Delta(\Delta G)$, is ~0.7 kcal mol$^{-1}$ under these conditions (Table II). To exclude the possibility that these small differences of $\Delta T_m$ = 4.8 °C and $\Delta(\Delta G)$ = 0.7 kcal mol$^{-1}$ could arise from the presence of the extra N-terminal Met in BPTI(G36S) (Figure 2), we repeated the measurements using recombinant wild-type BPTI containing Met in position 0. Within the experimental accuracy, identical data were obtained for native and recombinant wild-type BPTI.

*Binding Affinity of BPTI(G36S) for Proteinases.* As a further test of the structural integrity of the mutant protein, BPTI and BPTI(G36S) were assayed for their ability to inhibit bovine trypsin, human plasmin, and human kallikrein by measuring the hydrolytic activities of preincubated samples, as described under Materials and Methods. As can be seen

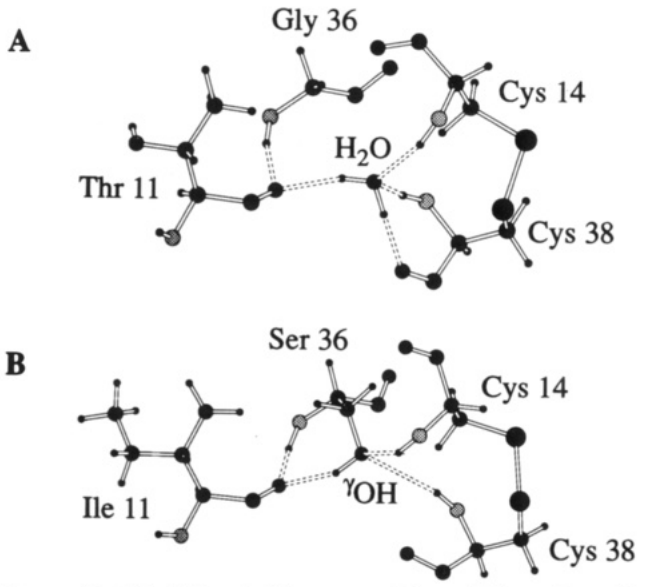


FIGURE 5: (A) Ball-and-stick representation of the amino acid residues involved in hydrogen bonding to the internal water molecule W122 (see Figure 1) in the crystal structure of BPTI form II (Wlodawer et al., 1984). (B) Same representation of the corresponding residues forming hydrogen bonds with the hydroxyl group of Ser 36 in the solution structure of toxin K (Berndt et al., 1993). Hydrogen bonds are indicated by dotted lines connecting the donor and acceptor atoms. For the sake of illustration, the hydrogen bond HN Cys 38/$\gamma$O Ser 36 is shown in panel B although it exceeds the standard criterion for the donor-acceptor distance by 0.3 Å (see text). A structure-type identical to that in panel B is implicated by the present NMR data for BPTI(G36S) (Figure 4), where Ile 11 is replaced by Thr as in panel A. Carbon atoms, black; oxygen, darkly hatched; nitrogen, lightly hatched; hydrogen, small, lightly hatched; sulfur, large, darkly hatched.

Table III: Equilibrium Constants, $K_i$ (mol/L), of Enzyme–Inhibitor Complexes

| enzyme | BPTI | BPTI(G36S) |
|---|---|---|
| trypsin (bovine pancreas) | $<1 \times 10^{-11}$ | $2 \times 10^{-11}$ |
| plasmin (human) | $9 \times 10^{-11}$ | $8 \times 10^{-8}$ |
| plasma kallikreine (human) | $3 \times 10^{-8}$ | $>5 \times 10^{-7}$ |

from Table III, the equilibrium constants, $K_i$, of the enzyme–inhibitor complexes are reduced by factors up to about 900 for the different enzymes when BPTI(G36S) is compared with BPTI. Within the range described under Materials and Methods, protease inhibition was independent of the incubation time used in the assay.

## CONCLUSIONS

The conformation-dependent dispersion of the $^1$H chemical shifts in globular proteins (Wüthrich, 1976) makes this parameter a highly sensitive probe of conformational differences between related proteins. Therefore, the data in Figure 3 convincingly demonstrate that the global structures of BPTI(G36S) and BPTI are nearly identical, with the sole noticeable deviations in the polypeptide segments 11–18 and 34–41, which are both spatially close to the mutation site at position 36 (Figures 1 and 2). The NMR data presented in Table I and Figure 4 convincingly demonstrate that the single interior hydration water molecule located in this loop in BPTI has been replaced by the serine hydroxyl group in the mutant BPTI(G36S), analogous to the situation in toxin K. The slightly reduced stability of BPTI(G36S) relative to BPTI, with $\Delta(\Delta G) \approx 0.7$ kcal mol$^{-1}$, can be accounted for by the loss of a hydrogen bond due to the fact that a hydroxyl moiety can donate only one proton to potential acceptor atoms, while a water molecule can donate two protons (Figure 5). The experimental data would also indicate that the significantly reduced affinity of BPTI(G36S) for binding to the serine proteinases trypsin, kallikrein, and plasmin (Table II) should be rationalized by strictly localized structural differences near the mutation site.

The residues 11–18 and 34–41, which have significant chemical shift differences between the two proteins (Figure 3), are nearly identical to those directly involved in the intermolecular contacts between BPTI and kallikrein in the BPTI–kallikrein complex (Chen & Bode, 1983), and these are also the residues coordinating the internal water molecule W122 (Figure 1). Although it is therefore a priori not surprising that even minor structural rearrangements of this region could adversely affect the binding affinity, no detailed explanation can be given based on the available data. Some time ago, Dufton (1985) advanced the hypothesis that replacement of the strictly conserved Gly 36 in Kunitz-type proteinase inhibitors might be a major factor in abolishing inhibitory binding in dendrotoxins, besides the substitution of Gly/Ala 16 by a charged or polar residue (Figure 2). As a possible rationale, he suggested that Ser 36 might compete with Ser 195 of the enzyme for hydrogen bonding to His 57 of the enzyme, but molecular modeling has shown that the side chain of His 57 would be too far away from the side chain of residue 36 in the inhibitor to take part in direct interactions without concomitant significant structural changes in the enzyme (Skarzinsky, 1992). The presently observed large decrease in binding affinity of the mutant BPTI(G36S) when compared to wild-type BPTI suggests that structure determinations of the relevant proteinase–inhibitor complexes might be of considerable interest as a basis for further discussions on this point.

Another recently described single-point mutation in BPTI, BPTI(Y36G), was found to cause more extensive changes of the protein structure, with backbone atom displacements greater than 2.0 Å relative to BPTI. In concert, none of the four internal water locations are conserved, being replaced by three new internal hydration water molecules that stabilize the altered conformation (Housset et al., 1991). This observation and the results on BPTI(G36S) presented in this paper underscore the importance of satisfying hydrogen-bond requirements in the protein interior, and a tolerance of the protein architecture to accept a limited number of internal hydration water molecules for this purpose. The manipulation of cavities by introduction or displacement of internal hydration water molecules might thus become an intriguing additon to the repertoire of biochemists involved in protein design and protein engineering (e.g., Loewenthal et al., 1992; Nicholson et al., 1988).

## ACKNOWLEDGMENT

We thank J. Ebbers and H. D. Hörlein (Bayer AG) for carrying out the cloning and the purification of the protein and R. Marani (ETH) for the careful processing of the manuscript.

## REFERENCES

Baker, E. N., & Hubbard, R. E. (1984) *Prog. Biophys. Mol. Biol. 44*, 97–179.

Becktel, W. J., & Schellman, J. A. (1987) *Biopolymers 26*, 1859–1877.

Berndt, K. D., Güntert, P., Orbons, L. P. M., & Wüthrich, K. (1992) *J. Mol. Biol. 227*, 757–775.

Berndt, K. D., Güntert, P., & Wüthrich, K. (1993) *J. Mol. Biol.* (submitted).

Brown, L. R., DeMarco, A., Richarz, R., Wagner, G., & Wüthrich, K. (1978) *Eur. J. Biochem. 88*, 87–95.
Chazin, W., & Wright, P. E. (1988) *J. Mol. Biol. 202*, 623–636.
Chen, Z., & Bode, W. (1983) *J. Mol. Biol. 164*, 283–311.
Clore, G. M., Bax, A., Wingfield, P. T., & Gronenborn, A. M. (1990) *Biochemistry 29*, 5671–5676.
Das, R. C., Shultz, J. L., & Lehman, D. J. (1989) *Mol. Gen. Genet. 218*, 240–248.
Deisenhofer, J., & Steigmann, W. (1975) *Acta. Crystallogr. B 31*, 238–250.
Dill, K. A. (1987) *Biochemistry 29*, 7133–7155.
Dufton, M. J. (1985) *Eur. J. Biochem. 153*, 647–654.
Empie, M. W., & Laskowski, M. (1982) *Biochemistry 21*, 2274–2284.
Forman-Kay, J. D., Gronenborn, A. M., Wingfield, P. T., & Clore, G. M. (1991) *J. Mol. Biol. 220*, 209–216.
Güntert, P., & Wüthrich, K. (1992) *J. Magn. Reson. 96*, 403–407.
Housset, D., Kim, K. S., Fuchs, J., Woodward, C., & Wlodawer, A. (1991) *J. Mol. Biol. 220*, 757–770.
Kauzmann, W. (1959) *Adv. Protein Chem. 14*, 1–63.
Kraulis, P. J. (1991) *J. Appl. Crystallogr. 24*, 946–950.
Liepinsh, E., Otting, G., & Wüthrich, K. (1992) *J. Biomol. NMR 2*, 447–465.
Loewenthal, R., Sancho, J., & Fersht, A. R. (1992) *J. Mol. Biol. 224*, 759–770.
Marion, D., & Wüthrich, K. (1983) *Biochem. Biophys. Res. Commun. 113*, 967–974.
Némethy, G., & Scheraga, H. A. (1977) *Q. Rev. Biophys. 10*, 239–352.
Nicholson, H., Becktel, W. J., & Matthews, B. W. (1988) *Nature 336*, 651–656.
Nozaki, Y. (1972) in *Methods in Enzymology* (Hirs, C. W. H., & Timasheff, S. N., Eds.) Vol. 26, p 43, Academic Press, New York.
Otting, G., & Wüthrich, K. (1989) *J. Am. Chem. Soc. 111*, 1871–1875.
Otting, G., Liepinsh, E., & Wüthrich, K. (1991a) *J. Am. Chem. Soc. 113*, 4363–4364.
Otting, G., Liepinsh, E., Farmer, B. T., & Wüthrich, K. (1991b) *J. Biol. NMR 1*, 209–215.
Otwinowski, Z. O., Schevitz, R. W., Zhang, R. G., Lawson, C. L., Joachimiak, A., Marmorstein, R. Q., Luisi, B. F., & Sigler, P. B. (1988) *Nature 335*, 321–329.
Richardson, J. (1981) *Adv. Protein Chem. 34*, 167–339.
Sambrook, J., Fritsch, E. F., & Maniatis, T. (1989) *Molecular Cloning*, Cold Spring Harbor Laboratory Press, Cold Spring Harbor, NY.
Skarzynski, T. (1992) *J. Mol. Biol. 224*, 671–683.
Strydom, D. J. (1973) *Nature New Biol. 243*, 88–89.
Tanford, C. (1962) *J. Am. Chem. Soc. 84*, 4240–4247.
Tüchsen, E., & Woodward, C. (1987) *Biochemistry 26*, 1918–1925.
Wlodawer, A., Walter, J., Huber, H., & Sjölin, L. (1984) *J. Mol. Biol. 180*, 301–329.
Wlodawer, A., Nachman, J., Gilliland, G. L., Gallagher, W., & Woodward, C. (1987) *J. Mol. Biol. 198*, 469–480.
Wüthrich, K. (1976) *NMR in Biological Research: Peptides and Proteins*, North Holland, Amsterdam.
Wüthrich, K. (1986) *NMR of Proteins and Nucleic Acids*, Wiley, New York.